

CASE REPORT

Open Access



Anlotinib treatment for rapidly progressing pediatric embryonal rhabdomyosarcoma in the maxillary gingiva: a case report

Bo Ding^{1†}, Biwei Mai^{1†}, Tingyan Liu^{2†}, Cuicui Liu³, Hairong Bao³, Jingzhou Hu⁴, Xiaowen Qian⁵, Song Wang³, Qiuxiang Ou³, Xiujuan Dong⁶, Zhixian Lei^{1*} and Gangfeng Yan^{2*}

Abstract

Background Embryonal rhabdomyosarcoma (ERMS) is a highly aggressive form of soft-tissue sarcoma that predominantly affects children. Due to limited benefits and resistance to therapy, there is an unmet need to explore alternative therapeutic strategies.

Case presentation In this report, we present a rare case of pediatric ERMS located on the right side of the maxillary gingiva. A composite reference guide integrating clinical, radiographic, and histopathologic findings was used for a definitive diagnosis. Targeted next-generation sequencing of tumor biopsy was performed to identify genetic alterations. A 12-year-old female was admitted to the Pediatric Intensive Care Unit (PICU) and underwent a tracheotomy to relieve asphyxiation caused by a 5.5 cm diameter mass compressing the tongue root and pharyngeal cavity. Hematoxylin and eosin staining revealed a hybrid morphology characterized by clusters of round and spindle cells. Further immunohistochemistry assays indicated positive immunoreactivity for desmin, myogenin, and MyoD1. Various genetic alterations were identified, including mutations in *GNAS*, *HRAS*, *LRP1B*, amplification of *MDM2* and *IGF1R*, and two novel *IGF1R* fusions. Negative *PAX-FOXO1* fusion status supported the clinical diagnosis of ERMS. Initial treatment involved standard chemotherapy; however, the tumor persisted in its growth, reaching a maximum volume of 12 cm × 6 cm × 4 cm by the completion of treatment. Subsequent oral administration of anlotinib yielded a significant antitumor response, characterized by substantial tumor necrosis and size reduction. Following the ligation of the tumor pedicle and its removal, the patient developed a stabilized condition and was successfully discharged from PICU.

Conclusions Our study highlights the importance of accurate diagnosis established on multifaceted assessment for the effective treatment of ERMS. We present compelling evidence supporting the clinical use of anlotinib as a promising treatment strategy for pediatric ERMS patients, especially for those resistant to conventional chemotherapy.

Keywords Embryonal rhabdomyosarcoma, Maxillary gingiva, Anlotinib, Chemotherapy, Tyrosine kinase inhibitor

[†]Bo Ding, Biwei Mai and Tingyan Liu contributed equally to this work.

*Correspondence:
Zhixian Lei
leix698@163.com
Gangfeng Yan
gangfeng_yan@fudan.edu.cn

Full list of author information is available at the end of the article



© The Author(s) 2024. **Open Access** This article is licensed under a Creative Commons Attribution-NonCommercial-NoDerivatives 4.0 International License, which permits any non-commercial use, sharing, distribution and reproduction in any medium or format, as long as you give appropriate credit to the original author(s) and the source, provide a link to the Creative Commons licence, and indicate if you modified the licensed material. You do not have permission under this licence to share adapted material derived from this article or parts of it. The images or other third party material in this article are included in the article's Creative Commons licence, unless indicated otherwise in a credit line to the material. If material is not included in the article's Creative Commons licence and your intended use is not permitted by statutory regulation or exceeds the permitted use, you will need to obtain permission directly from the copyright holder. To view a copy of this licence, visit <http://creativecommons.org/licenses/by-nc-nd/4.0/>.

Background

Rhabdomyosarcoma (RMS) is a highly malignant soft-tissue sarcoma (STS) of mesenchymal origin [1]. RMS is most prevalent in children under 10 years, appearing as an aggressive soft-tissue mass in the head and neck, genitourinary system, and extremities. Oral lesions are uncommon, accounting for only 10-12% of head and neck RMS cases, with a predilection for the palate, tongue, lips, and buccal mucosa [2]. The World Health Organization classification of soft tissue tumors categorizes RMS into four major histological subtypes, including embryonal, alveolar, pleomorphic, and spindle cell/sclerosing rhabdomyosarcoma [3]. Embryonal rhabdomyosarcoma (ERMS) is the predominant subtype accounting for approximately 60% of all cases, followed by alveolar rhabdomyosarcoma (ARMS) in about 30% [4].

Histopathology stands as the gold standard for diagnosing and grading soft tissue tumors, albeit consistent correlations between radiological and pathological findings and molecular testing are crucial for both diagnostic accuracy and prognostic relevance. Morphologically, most primitive rhabdomyoblasts are stellate cells characterized by a sparsity of amphophilic cytoplasm. As these cells undergo differentiation, they manifest a transition towards a more eosinophilic cytoplasm and adopt an elongated morphology, leading to the formation of myotubes and cross-striations [5]. While tumor cells from different RMS subtypes commonly exhibit diffuse positivity for desmin, a protein indicative of muscle differentiation, transcription factors associated with rhabdomyogenic differentiation, such as myogenin and myogenic differentiation 1 (MyoD1), demonstrate heterogeneous staining patterns [6]. Moreover, the molecular characteristics of RMS subtypes significantly vary, which is essential for confirming the diagnosis. The majority of ARMS harbor *FOXO1* fusions, whereas ERMS displays a heterogeneous genomic profile and is distinguished by the absence of *PAX-FOXO1* fusions.

The mainstay treatment approach for RMS includes a combination of surgery and radiotherapy. In cases where surgery is no longer an option, a multimodal chemotherapy regimen using vincristine, actinomycin D, and cyclophosphamide is commonly employed to extend the patient's survival. However, given its toxicity and limited overall survival benefits, there is an urgent need to develop therapies that offer improved survival outcomes while maintaining acceptable safety profiles. Tumor angiogenesis is one of the important processes in tumorigenesis and metastasis. To date, several anti-angiogenic agents, encompassing bevacizumab, pazopanib, enavatinib, sunitinib, and apatinib, have been approved for the treatment of various cancers. Anlotinib, a novel oral multi-targeted receptor tyrosine kinase inhibitor (TKI), has demonstrated encouraging antitumor efficacy and

acceptable toxicity in treating various human cancers by blocking the vascular endothelial growth factor receptor (VEGFR), fibroblast growth factor receptor (FGFR), and platelet-derived growth factor receptor (PDGFR) pathways. Notably, anlotinib was approved by the China Food and Drug Administration (CFDA) as a second-line treatment therapy for advanced STS [12]. While anlotinib has been reported for use in adult patients with relapsed refractory RMS, there is little research on pediatric sarcomas. Further investigation is warranted to evaluate the efficacy and safety of anlotinib in pediatric cancers.

Here, we present a rare case of a 12-year-old female diagnosed with ERMS, whose tumor located in the maxillary gingiva aggressively progressed followed by standard chemotherapy. Oral administration of anlotinib demonstrated significant antitumor activity, leading to a stabilization of the patient's condition.

Case presentation

In August 2023, a 12-year-old female was admitted to the Pediatric Intensive Care Unit (PICU) with an approximately 5 cm diameter mass and painful swelling in the maxillary gingiva (Fig. 1A). To address asphyxiation caused by compression of the tongue root and pharyngeal cavity, a tracheotomy was performed under local anesthesia. The lesion, initially observed about a month ago, is characterized by unexplained swelling on the right side of the gingiva accompanied by surface ulceration and discomfort. The patient had received four days of anti-infective therapy at a local community hospital before hospitalization; however, the swelling worsened rapidly.

Physical examination of the patient revealed normal vital signs, with a temperature of 36.6 °C. No craniofacial deformities, orbital depression, or eyelid edema were observed. Intraoral examination disclosed an approximately 5 cm diameter mass, accompanied by tongue compression, restricted mouth opening, and purulent secretions attached to its surface (Fig. 1A). There were no signs of bleeding or exudate around the tracheotomy site, and the tracheal cannula remained in place. Laboratory examinations, including blood glucose levels, complete blood count, blood chemistry, urinalysis, urine biochemistry, and thyroid function tests, yielded normal results.

Maxillofacial magnetic resonance imaging (MRI) scans revealed a 5.5 cm × 4.7 cm × 5 cm mass in the parapharyngeal space, with extension to the oral cavity (Fig. 1B-G). Bilateral inflammation of the maxillary sinuses and multiple enlarged lymph nodes in the neck and submandibular regions were also observed. Diffusion-weighted imaging (DWI) indicated restricted diffusion within the mass, with associated bone destruction and compression of the tongue's root (Fig. 1H, I). No abnormalities were detected in the chest, abdomen, pelvis, musculoskeletal system, or spinal cord. Comprehensive assessments of

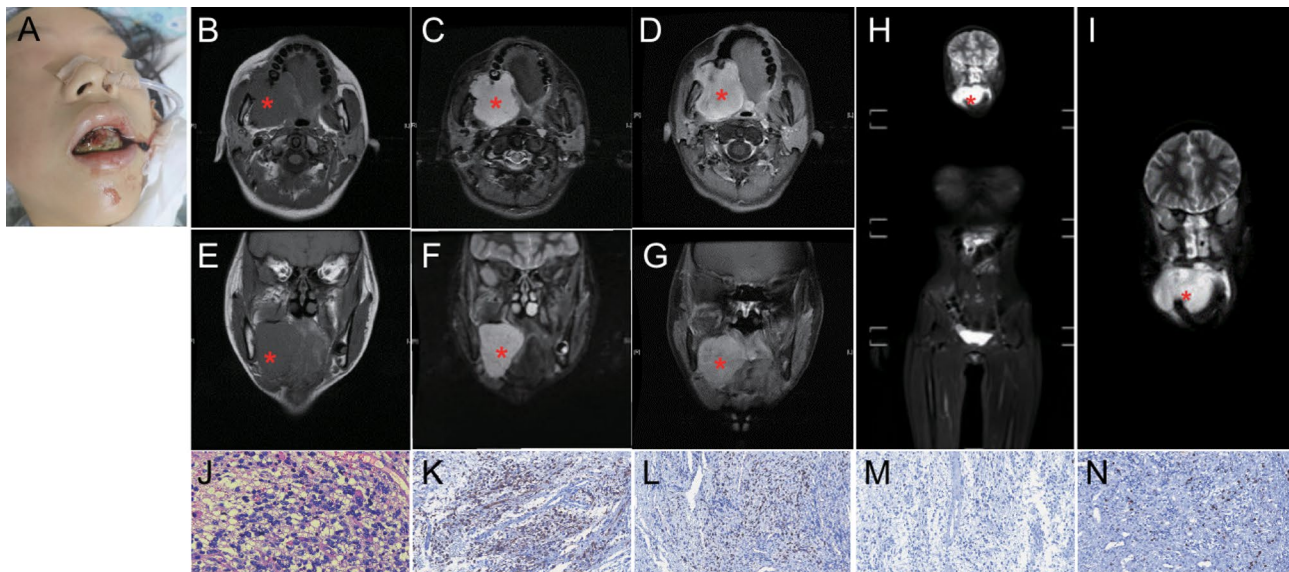


Fig. 1 Comprehensive diagnostic approach facilitates the definitive diagnosis of ERMS. **(A)** Clinical presentation of the soft-tissue mass within the oral cavity. **(B-D)** Axial magnetic resonance imaging (MRI) of T1 (B), T2 (C), and contrast-enhanced (D) scans revealed a 5.5 cm × 4.7 cm × 5 cm mass (asterisk) in the right maxilla upon admission. **(E-G)** Coronal MRI presents T1 (E), T2 (F), and contrast-enhanced (G) scans of the mass (asterisk). **(H-I)** Diffusion-weighted imaging revealed a tumor mass (asterisk) located in the right maxillofacial region, accompanied by adjacent bone destruction and compression of the tongue root. **(J)** A hyperplastic lesion characterized by small blue round cell tumor proliferation was identified within the mucosa propria through hematoxylin and eosin staining (400x). The cellular envelope exhibited vacuolation and intense brightness, while nuclear atypia, elevated nucleo-plasma ratio, and evident nuclear division were observed. Interstitial blood vessels displayed marked abundance, concomitant with conspicuous endothelial cell proliferation and focal areas of infarction. **(K-N)** Immunohistochemistry staining (200x) shows positive staining of desmin (K), MyoD1 (L), myogenin (M), and Ki67 (N) in the tumor biopsy

thyroid, liver, and kidney function, cardiac enzymes, electrolytes, and coagulation profiles exhibited no significant abnormalities. Additionally, color ultrasounds of hepatobiliary, pancreatic, splenic, urinary, and cardiac systems displayed no structural irregularities. Cerebrospinal fluid analyses, including routine examination, biochemistry, smear, and culture, yielded normal results. Furthermore, bone marrow aspiration indicated active hyperplasia across three lineages, notably increased proportion in the red cell lineage. The findings from both the bone marrow aspiration and lumbar puncture did not support intracranial or bone metastasis.

The hematoxylin and eosin (H&E) staining of the gingival mass biopsy revealed features suggestive of small round blue cell tumor-like hyperplasia within the lamina propria of the tumor mucosa. The cells displayed empty cytoplasm, notable nuclear atypia, a high nuclear-cytoplasmic ratio, and frequent mitoses (Fig. 1J). Additionally, abundant interstitial blood vessels, endotheliocytosis, and areas of necrosis were observed. Further immunohistochemistry (IHC) analysis demonstrated diffusely positive staining for desmin and MyoD1, and scatter positivity for myogenin (Fig. 1K-N). Ki67 was also positive with a proliferation index of 20%. Therefore, based on a composite reference combining clinical, radiological, and histopathological findings, the patient was diagnosed with pediatric ERMS occurring in the maxillary gingiva.

Molecular assessment of the tumor biopsy was conducted using targeted next-generation sequencing (NGS) against 437 cancer-related genes using the GeneSeqPrime™ panel (Supplementary Information). This unveiled various genetic alterations, including missense mutations in *GNAS* and *HRAS*, a frameshift mutation in *LRP1B*, amplification of *MDM2* and *IGF1R*, and two translocations in the *IGF1R* gene (Table 1). On the other hand, the absence of *PAX~FOXO1* gene fusions further confirmed the definitive diagnosis of ERMS in this patient. Additionally, the tumor mutation burden was determined to be 3.1 mutations/Mb, with a microsatellite stable status. IHC analysis indicated positive expression of programmed death ligand 1 (PD-L1), with a combined positive score (CPS) of 3.

As chemotherapy remains the mainstay treatment for ERMS, the patient underwent a two-week consecutive chemotherapy regimen, including the administration of vincristine (1.5mg/m² on days 1 and 8), actinomycin D (0.045/m² on day 1), and cyclophosphamide (1.2 g/m² on day 1) (Fig. 2A). Upon treatment initiation, the patient developed a fever of up to 39.0 °C, accompanied by cough and sputum rattling, thrombocytopenia, and elevated C-reactive protein levels. Sputum culture confirmed the presence of lung infection, prompting sequential anti-infective therapy with ceftriaxone, cefoperazone-sulbactam, and oxacillin. Despite the effective control of

Table 1 Genetic alterations identified by targeted next-generation sequencing

Gene	Vari- ant type	Mutation	AA change	Copy number	Allele fre- quency
<i>GNAS</i>	Mis- sense muta- tion	c.601 C>T	p.R201C		30.4%
<i>HRAS</i>	Mis- sense muta- tion	c.35G>A	p.G12D		31.9%
<i>LRP1B</i>	Frame- shift muta- tion	c.4351del	p.S1451Qfs*9		23.9%
<i>IGF1R</i>	Am- plifica- tion	~	~	103.7	
<i>MDM2</i>	Am- plifica- tion	~	~	33.6	-
<i>IGF1R</i>	Trans- loca- tion	<i>LRRC28~IGF1R</i> (exon 6: exon 19)	<i>LRRC28~IGF1R</i>		0.1%
<i>IGF1R</i>	Trans- loca- tion	<i>IGR~IGF1R</i> (upstream <i>SYNM</i> : exon 21)	<i>IGR~IGF1R</i>		1.0%

Abbreviations: AA, amino acid; *GNAS*, G protein subunit alpha 5; *HRAS*, HRas proto-oncogene, GTPase; *LRP1B*, LDL receptor related protein 1B; *IGF1R*, insulin like growth factor 1 receptor; *IGR*, intergenic region

the patient's temperature and infection parameters, the tumor continued to grow, reaching a maximum volume of 12 cm × 6 cm × 4 cm by the completion of chemotherapy (Fig. 2B-D).

To control rapid tumor growth, anlotinib was administered to the patient in a 2-week on/1-week off scheme for two cycles. Specifically, the patient received oral anlotinib at a starting dose of 10 mg once daily (qd) during the first week of treatment, while the dose was escalated to 12 mg qd during the second week. No abnormalities in blood routine examination, blood biochemistry, and thyroid function were observed throughout the treatment period. Remarkably, the tumor size underwent a significant reduction during treatment, with necrosis and tissue detachment becoming evident after the first cycle of anlotinib therapy (Fig. 2E-H). The reduction in tumor size was further confirmed by an enhanced computed tomography scan after the initial treatment cycle (Fig. 2I). Subsequently, the tumor pedicle was ligated with sutures the following day, and the tumor was successfully excised without massive bleeding (Fig. 2J-L). Throughout this process, the patient did not develop a fever or experience breathing or feeding difficulties.

Residual tumor tissues were still visible in the upper gum upon intraoral examination, prompting the patient to undergo a second cycle of anlotinib treatment at a dose of 12 mg qd. Throughout the treatment regimen, no instances of hypertension or gastrointestinal reactions were reported. Routine monitoring of blood, liver, and kidney function revealed no abnormalities, except for an elevation in thyroid stimulating hormone levels, a known treatment-related adverse effect [7]. Despite an unevenly enhanced intraoral mass shadow observed in the CT scan, the lateral extended mass was not visible (Fig. 2M). With a stabilized condition, the patient was successfully discharged from the hospital on September 28, 2023.

Discussion and conclusions

In this report, we present a rare case of pediatric ERMS, in which the primary tumor manifested in the maxillary gingiva and exhibited rapid progression after chemotherapy. Oral administration of anlotinib, a multi-targeted TKI, showcased notable antitumor efficacy, leading to the patient's discharge upon stabilization.

ERMS is the predominant histological subtype of rhabdomyosarcoma, primarily presenting as an aggressive soft-tissue mass in the head and neck, genitourinary system, and extremities of children. Neoplasms in the oral cavity are rarely reported, potentially leading to missed or late disease recognition. Considering the aggressive nature of the tumor, it is pivotal to obtain a definitive diagnosis as early as possible for an optimal treatment outcome and prolonged patient survival. Currently, histopathology remains the gold standard for diagnosing soft-tissue tumors. Nevertheless, a combination of clinical, radiographic, and histopathologic findings is crucial for an accurate diagnosis and distinguishing between ERMS and other histological subtypes. In this case, we established a composite reference guide, integrating clinical presentations, radiological images, morphological features, and IHC findings. Additionally, with the recent advances and better understanding of molecular genetics, notably the lack of *FOXO1* fusion as the major characteristic of ERMS, we confirmed the presence of ERMS in this patient, notwithstanding its less frequently reported oral location. Owing to the prompt diagnosis, the patient demonstrated a significant response to anlotinib treatment, leading to successful tumor reduction and removal while maintaining a stabilized condition of the patient.

Leveraging targeted NGS, we identified numerous somatic genomic variants from the tumor biopsy of the patient, which provided insights into the development of precision-based targeted therapy for ERMS. Prior studies have uncovered several implied molecular features of ERMS, such as *p53* loss [8], RAS pathway activation [9], and *MYOD1* mutation [10]. Consistently, the patient was found to harbor a somatic *HRAS* p.G12D mutation,

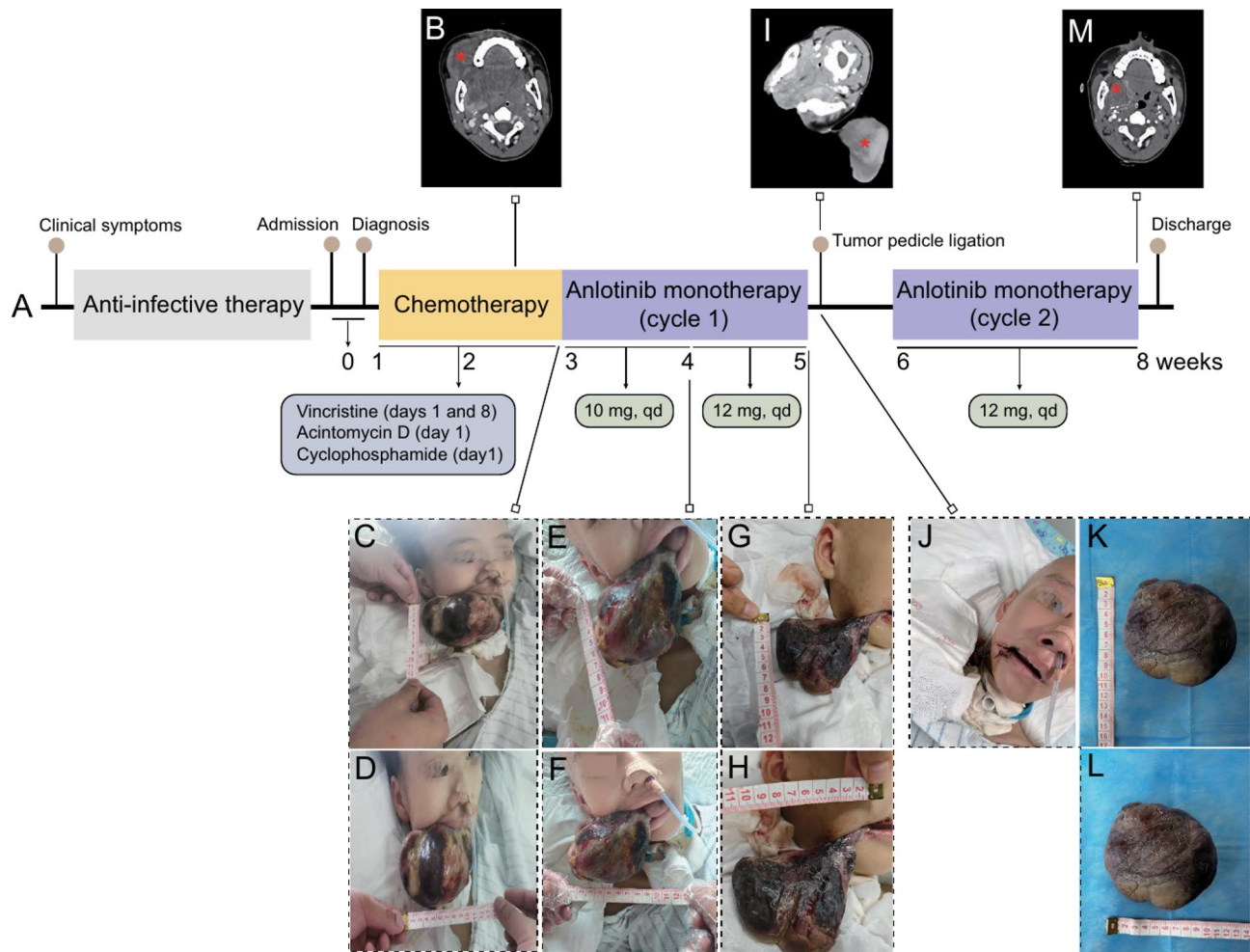


Fig. 2 Anlotinib treatment resulted in a reduction in tumor size. **(A)** The patient's treatment plan involved oral administration of anlotinib in a two-week on/one-week off regimen following chemotherapy to control the rapidly progressing tumor. Anlotinib was initially given at 10 mg once daily (qd) for the first week, increasing to 12 mg qd for the second week of the first cycle. Subsequent cycles maintained the dose at 12 mg qd. **(B)** Contrast-enhanced computed tomography (CT) scan revealed a 10 cm × 6.2 cm irregular mass (asterisk) occupying the right side of the oral cavity, presenting malignant features with abundant blood supply. Complete obstruction of the oral-pharyngeal passage, nasal-pharyngeal stenosis, and metastasis to surrounding lymph nodes. **(C-H)** Tumor appearance and size measurements at the beginning (C, D), at the first week of treatment (E, F), and after the first anlotinib treatment cycle (G, H). **(I)** CT scan showed a significantly reduced 7.6 cm × 2.0 cm intraoral mass (asterisk) after anlotinib treatment, with blood supply mainly from the right arterial/lingual artery. **(J-L)** Clinical presentation of the patient and tumor mass following tumor pedicle ligation at the end of the first cycle of anlotinib treatment. **(M)** CT scan showed an unevenly enhanced mass shadow on the right side of the oral cavity (asterisk), indicating abundant blood supply and numerous small blood vessels, with the lateral extended mass being invisible after tumor removal

which has been known as an oncogenic mutation exhibiting sensitivity to tipifarnib in bladder urothelial carcinoma and head and neck squamous cell carcinoma [11, 12]. Additionally, we also identified *MDM2* amplification from the tumor biopsy, which has been observed in approximately 0–10% of RMS cases [13]. Indeed, *MDM2* is a key regulator of the tumor suppressor p53, and its overexpression is associated with resistance to chemotherapy in human malignancies. We reasoned that the presence of *MDM2* amplification might serve as a plausible explanation for the unexpectedly rapid progression of the primary tumor following the multimodal chemotherapy regimen. Furthermore, while the tumor was negative

for *FOXO1* fusions, we identified two novel fusion events and a gene amplification involving the *IGF1R* gene. *IGF1R* amplification has been reported in both ERMS and ARMS [14]. *IGF1R* has been known for its role in tumorigenesis and growth by serving as important activators of the AKT and mitogen-activated protein kinase (MAPK) signaling networks in neoplastic tissues [15]. Several clinical trials are ongoing to investigate the therapeutic potential of *IGF1R* monotherapy or combination therapy with other small-molecule inhibitors or chemotherapy in refractory sarcoma patients [16–19].

Anlotinib is an orally available, highly potent, multitargeted TKI that blocks VEGF, FGFR, and PDGFR

pathways. The ALTER0203 trial demonstrated promising efficacy and acceptable toxicity of anlotinib in advanced soft-tissue sarcoma patients who had failed standard chemotherapy, leading to CFDA approval for its use in the treatment of advanced STS [20, 21]. However, there have been limited reports on the use of anlotinib in treating refractory or recurrent pediatric solid tumors. Lu et al. retrospectively analyzed 41 patients with heavily pre-treated pediatric solid tumors, of whom 12 were diagnosed with RMS [22]. For these patients, anlotinib with or without combined chemotherapy showcased a disease control rate of 65.9% (27/41), median progression-free survival of 2.87 months (95% confidence interval: 0.86–4.88), as well as tolerable adverse events. Additionally, a phase 1 study is currently ongoing to investigate the toxicity and pharmacokinetic profile of anlotinib in pediatric patients with recurrent or refractory sarcomas, focusing on RMS as the major subtype of cancer [23]. To the best of our knowledge, we are the first to report such a remarkable short-term clinical outcome of a pediatric ERMS patient whose tumor experienced significant size reduction after anlotinib treatment. It is also worth noting that the patient tested positive for PD-L1 expression with a CPS score of 3. A phase 2 study showcased promising treatment efficacy and manageable toxicity when anlotinib was combined with TQB2450, a novel PD-L1 antibody, in advanced/metastatic soft-tissue sarcoma [24]. In another case study, a male patient who failed multiple lines of treatment achieved a partial response following toripalimab and anlotinib combined therapy [25]. Collectively, these encouraging results suggest a potential treatment strategy involving the combination of anti-PD-(L)1 therapies and anlotinib for our patient if she experiences tumor relapse in the future.

In conclusion, we present an interesting case of a pediatric ERMS located in the oral cavity, exhibiting resistance to standard chemotherapy but remaining sensitive to anlotinib monotherapy. The case highlighted the importance of accurate diagnosis established on multi-faceted assessment for effective treatment. Furthermore, comprehensive genomic profiling revealed potential actionable targets for ERMS patients.

Abbreviations

ARMS	alveolar rhabdomyosarcoma
CPS	combined positive score
DWI	Diffusion-weighted imaging
ERMS	embryonal rhabdomyosarcoma
FOXO1	Forkhead Box O1
FGFR	fibroblast growth factor receptor
H&E	hematoxylin and eosin
IHC	immunohistochemistry
IGF1R	insulin like growth factor 1 receptor
RMS	rhabdomyosarcoma
MRI	magnetic resonance imaging
MyoD1	myogenic differentiation 1
NGS	next-generation sequencing
PICU	Pediatric Intensive Care Unit

PD-L1	programmed death ligand 1
PDGFR	platelet-derived growth factor receptor
qd	once daily
TKI	tyrosine kinase inhibitor
VEGFR	vascular endothelial growth factor receptor

Supplementary Information

The online version contains supplementary material available at <https://doi.org/10.1186/s13000-024-01555-5>.

Supplementary Material 1

Acknowledgements

We thank the patient and her family members for providing consent to present the data in this study.

Author contributions

BD, BWM, and TYL designed the study. BD, BWM, TYL, JZH, XWQ, and XJD acquired clinical data and performed patient follow-ups. BD, BWM, and TYL wrote the manuscript. CCL, HRB, SW, and QXO edited the manuscript. ZXL and GFY supervised the study. All authors read and approved the final manuscript.

Funding

Not applicable.

Data availability

All data generated or analyzed during this study are included in this published article and its supplementary information files.

Declarations

Ethics approval and consent to participate

The ethics approval was waived. The written informed consent form was obtained from the patient's parents. All methods were performed in accordance with the ethical standards as laid down in the Declaration of Helsinki and its later amendments or comparable ethical standards.

Consent for publication

Written informed consent to publish the clinical details and images were obtained from the patient's parents.

Competing interests

CCL, HRB, SW, and QXO are employees of Nanjing Geneseeq Technology Inc. The remaining authors declare no competing interests.

Author details

¹Department of Pediatric Intensive Care Unit, Hainan Women and Children's Medical Center, Children's Hospital of Fudan University at Hainan, Children's Hospital of Hainan Medical University, Haikou 570100, China

²Department of Pediatric Intensive Care Unit, National Center for Children's Health, Children's Hospital of Fudan University, 399 Wanyuan Road, Shanghai 201102, China

³Geneseeq Research Institute, Nanjing Geneseeq Technology Inc, Nanjing 210032, China

⁴Department of Oral and Maxillofacial Surgery, ZhangZhiyuan Academician Workstation, Hainan Western Central Hospital, Shanghai Ninth People's Hospital, Danzhou 571700, Hainan, China

⁵Department of Hematology and Oncology, Children's Hospital of Fudan University, National Children's Medical Center, Shanghai 201102, China

⁶Department of Hematology and Oncology, Hainan Women and Children's Medical Center, Children's Hospital of Fudan University at Hainan, Children's Hospital of Hainan Medical University, Haikou 570100, China

Received: 3 July 2024 / Accepted: 22 September 2024

Published online: 08 October 2024

References

1. Skapek Stephen X, Ferrari Andrea, Gupta Abha A, Lupo Philip J, Butler Erin S, Janet, et al. Rhabdomyosarcoma Nat Reviews Disease Primers. 2019;5(1):1.
2. Nangalia Richa S, Neha SM, Abdul, Mousumi P. Rhabdomyosarcoma involving Maxilla mimicking gingival enlargement: a diagnostic challenge. *BMJ Case Rep CP*. 2019;12(11):e230692.
3. Bansal A, Goyal S, Goyal A, Jana M. WHO classification of soft tissue tumours 2020: an update and simplified approach for radiologists. *Eur J Radiol*. 2021;143:109937.
4. Loeb D.M., Thornton K., Shokek O. Pediatric soft tissue sarcomas. *Surg Clin North Am*. 2008;88(3):615–27. vii.
5. Rong Fan DM, Parham LL, Wang. An Integrative Morphologic and Molecular Approach for Diagnosis and subclassification of Rhabdomyosarcoma. *Arch Pathol Lab Med*. 2022;146(8):953–9.
6. Morotti RA, Nicol KK, Parham DM, Teot LA, Moore J, Hayes J, et al. An immunohistochemical algorithm to facilitate diagnosis and subtyping of rhabdomyosarcoma: the children's Oncology Group experience. *Am J Surg Pathol*. 2006;30(8):962–8.
7. Han B, Li K, Zhao Y, Li B, Cheng Y, Zhou J, et al. Anlotinib as a third-line therapy in patients with refractory advanced non-small-cell lung cancer: a multicentre, randomised phase II trial (ALTER0302). *Br J Cancer*. 2018;118(5):654–61.
8. Perot G, Chibon F, Montero A, Lagarde P, de The H, Terrier P, et al. Constant p53 pathway inactivation in a large series of soft tissue sarcomas with complex genetics. *Am J Pathol*. 2010;177(4):2080–90.
9. Stratton MR, Fisher C, Gusterson BA, Cooper CS. Detection of point mutations in N-ras and K-ras genes of human embryonal rhabdomyosarcomas using oligonucleotide probes and the polymerase chain reaction. *Cancer Res*. 1989;49(22):6324–7.
10. Kohsaka S, Shukla N, Ameur N, Ito T, Ng CK, Wang L, et al. A recurrent neomorphic mutation in MYO1 defines a clinically aggressive subset of embryonal rhabdomyosarcoma associated with PI3K-AKT pathway mutations. *Nat Genet*. 2014;46(6):595–600.
11. Lee HW, Sa JK, Gualberto A, Scholz C, Sung HH, Jeong BC, et al. A phase II trial of Tipifarnib for patients with previously treated, metastatic urothelial carcinoma harboring HRAS mutations. *Clin Cancer Res*. 2020;26(19):5113–9.
12. Ho AL, Brana I, Haddad R, Bauman J, Bible K, Oosting S, et al. Tipifarnib in Head and Neck squamous cell carcinoma with HRAS mutations. *J Clin Oncol*. 2021;39(17):1856–64.
13. Taylor AC, Shu L, Danks MK, Poquette CA, Shetty S, Thayer MJ, et al. P53 mutation and MDM2 amplification frequency in pediatric rhabdomyosarcoma tumors and cell lines. *Med Pediatr Oncol*. 2000;35(2):96–103.
14. Bridge JA, Liu J, Qualman SJ, Suijkerbuijk R, Wenger G, Zhang J, et al. Genomic gains and losses are similar in genetic and histologic subsets of rhabdomyosarcoma, whereas amplification predominates in embryonal with anaplasia and alveolar subtypes. *Genes Chromosomes Cancer*. 2002;33(3):310–21.
15. Pollak M. Insulin and insulin-like growth factor signalling in neoplasia. *Nat Rev Cancer*. 2008;8(12):915–28.
16. Weigel B, Malempati S, Reid JM, Voss SD, Cho SY, Chen HX, et al. Phase 2 trial of cixutumumab in children, adolescents, and young adults with refractory solid tumors: a report from the Children's Oncology Group. *Pediatr Blood Cancer*. 2014;61(3):452–6.
17. Wagner LM, Fouladi M, Ahmed A, Krailo MD, Weigel B, DuBois SG, et al. Phase II study of cixutumumab in combination with temsirolimus in pediatric patients and young adults with recurrent or refractory sarcoma: a report from the Children's Oncology Group. *Pediatr Blood Cancer*. 2015;62(3):440–4.
18. Chugh R, Griffith KA, Davis EJ, Thomas DG, Zavala JD, Metko G, et al. Doxorubicin plus the IGF-1R antibody cixutumumab in soft tissue sarcoma: a phase I study using the TITE-CRM model. *Ann Oncol*. 2015;26(7):1459–64.
19. Weigel SMB, Anderson JAMESR, Parham D, Teot LA, Rodeberg DA, Yock TI, Shulkin BL, Hawkins DS. Early results from Children's Oncology Group (COG) ARST08P1: pilot studies of cixutumumab or temozolomide with intensive multiagent chemotherapy for patients with metastatic rhabdomyosarcoma (RMS). *J Clin Oncol*, 2015. 33: p. Number 15_suppl.
20. Lina Tang, Yonggang Wang, Jianjun Zhang, et al. Efficacy and safety of anlotinib in advanced soft tissue sarcoma: results from one of multi-centers in a phase IIB trial (ALTER0203). *JCO*. 2019;37:e22518. https://doi.org/10.1200/JCO.2019.37.15_suppl.e22518.
21. Yao YCY, Wang S, Huang G, Cai Q, Shang G, Wang G, Qu G, Wu Q, Jiang Y, Song J, Chen J, Zhu X, Cai Z, Bai C, Lu Y, Yu Z. Jingnan Shen, and Jianqiang Cai, *Anlotinib for metastasis soft tissue sarcoma: a randomized, double-blind, placebo-controlled and multi-centered clinical trial*. *JCO*. 2018;36:11503–11503.
22. Lu S, Hong Y, Chen H, Wu L, Sun F, Wang J, et al. The efficacy and safety of Anlotinib in Pediatric patients with refractory or recurrent solid tumors. *Front Pharmacol*. 2022;13:711704.
23. Suying Lu, Juan Wang, Feifei Sun, et al. Phase I study of anlotinib in pediatric patients with high-risk, recurrent, or refractory sarcomas. *JCO*. 2023;41:e23538. https://doi.org/10.1200/JCO.2023.41.16_suppl.e23538.
24. Liu Jiayong G, Tian T, Zhichao L, Shu X, Jie B, Chujie, et al. Phase II study of TQB2450, a novel PD-L1 antibody, in combination with anlotinib in patients with locally advanced or metastatic soft tissue sarcoma. *Clin Cancer Res*. 2022;28(16):3473–9.
25. Xiaogang S, Xinyu W, Jun Z, Yali X, Hao Z, Mian X et al. Next generation sequencing predicting clinical effect of immunotherapy on adult Rhabdomyosarcoma patient: a case report. *Medicine*, 2023. 102(21).

Publisher's note

Springer Nature remains neutral with regard to jurisdictional claims in published maps and institutional affiliations.